Int J Adv Manuf Technol (2011) 57:61–71
DOI 10.1007/s00170-011-3267-9

ORIGINAL ARTICLE

Effect of very high cutting speeds on shearing, cutting forces and roughness in dry turning of austenitic stainless steels

A. I. Fernández-Abia · J. Barreiro · L. N. López de Lacalle · S. Martínez

Received: 10 January 2011 / Accepted: 8 March 2011 / Published online: 15 April 2011

Abstract Behavior of austenitic stainless steels has been studied at very high cutting speeds. Turning tests were carried out using the AISI 303 austenitic stainless steel. In particular, the influence of cutting speed on tool wear, surface quality, cutting forces and chip geometry has been investigated. These parameters have been compared when performing machining at traditional cutting speeds (lower than 350 m/min) versus high cutting speeds. The analysis of results shows that the material undergoes a significant change in its behavior when machining at cutting speeds above 450 m/min, that favors the machining operation. The main component of cutting forces reaches a minimum value at this cutting speed. The SEM micrographs of the machined surfaces show how at the traditional cutting speeds the machined surfaces contain cavities, metal debris and feed marks with smeared material particles. Surfaces machined at high cutting speeds show evidence of material side flow, which is more evident at cutting speeds above 600 m/min. Tool wear is located at the tool nose radius for lower cutting speeds, whereas it slides toward the secondary edge when cutting speed increases. An analysis of chips indicates also an important decrement in chip thickness for cutting speeds above 450 m/min. This study concludes that there is an unexplored range of cutting speeds very interesting for high-performance machining. In this range, the behavior of stainless steels is very favorable although tool wear rate is also significant. Nevertheless, nowadays the cost of tool inserts can be considered as secondary when comparing to other operation costs, for instance the machine hourly cost for high-end multitasking machines.

Keywords Austenitic stainless steel · Turning · Tool wear · High-performance machining · High speed

A. I. Fernández-Abia · J. Barreiro (✉) · S. Martínez
Department of Manufacturing Engineering, University of León, Escuela de Ingenierías Industrial e Informática, 24071 León, Spain
e-mail: jbarg@unileon.es, joaquin.barreiro@unileon.es

A. I. Fernández-Abia
e-mail: aifera@unileon.es

S. Martínez
e-mail: smarp@unileon.es

L. N. López de Lacalle
Department of Mechanical Engineering, University of the Vasque Country, Escuela Técnica Superior de Ingeniería, Alameda de Urquijo s/n, 48013, Bilbao, Spain
e-mail: norberto.lzlacalle@ehu.es

1 Introduction

The main purpose of high-speed machining (HSM) is to increase the material removal rate (MRR) while keeping the quality of machined parts with regard to as-design specifications. The material removal rate for a turning operation is given by the product of cutting speed (V_c), feed rate (f_n), and depth of cut (a_p). Therefore, if an increase in productivity is desired then an increase in these three cutting parameters is required.

However, increment of feed rate leads to worse quality in machined surfaces. Also, increment in depth of cut also negatively affects roughness of parts and produces an increment of cutting forces. This phenomenon increases the risk of catastrophic failure of cutting tools, and it demands additional power and better structural

stiffness in machine tools. Therefore, machining with high values for feed rate and depth of cut is only possible when working with relative soft materials, such as aluminum, light alloys, or ferrous alloys.

On the contrary, the effects of increasing cutting speed are opposite to the former parameters. As demonstrated in some researches, increase in cutting speed improves surface finish while reducing the cutting forces [1–4]. The drawback behind the use of high cutting speeds is the adverse effect in tool life. The well-known equation of Taylor for tool life estimation and other similar equations such as that of Kronenberg and König–Depiereux point out that the cutting parameter with more influence over tool life is the cutting speed. However, regardless of the aforementioned drawback, the current trend is to use high-speed machining to improve productivity and surface finish of machined parts. The reason is that the hourly cost of modern turning centers or multitasking machines is very much higher than that of the tool.

High-performance machining is possible with new tool materials and improved coating technologies, such as the PVD technique or the lateral rotating ARC-Cathodes technology that allows to obtain multilayer and nanomultilayer coatings [5]. These coatings have extremely high nanohardness at very high toughness and extremely high heat resistance, properties required for the tools used in the machining at severe cutting conditions [6].

Other aspect to consider is that in HSM, the chip section is kept at a constant. That is, feed rate and depth of cut are fixed at constant values while cutting speed is optimized as means to reach the objectives of productivity and partly quality while maintaining an acceptable tool life.

The range of cutting speeds for machining with acceptable tool life is very broad, depending on the part material. For example, aluminum can be machined using cutting speeds around 8,000 m/min [7], whereas the range of high speed for titanium alloys or Inconel is around 250 m/min [8]. Traditionally, the machining of austenitic stainless steels is performed with cutting speeds between 150 and 350 m/min, that is, a moderate range. There are no available studies which consider the behavior of these steels when machining at higher cutting speeds.

Austenitic stainless steels are considered difficult materials for machining due to their high friction coefficient, low thermal conductivity, high coefficient of thermal expansion, high ductility, and high work-hardening rate [9]. The friction coefficient at the chip-tool interface is in general higher for stainless steels than for other steels. This fact leads to a faster degradation of cutting tools [10].

The low thermal conductivity implies an increase of temperature in the tool and, consequently, a reduction of tool life. The low thermal conductivity and the high work-hardening rate affect chip formation, which suffers catastrophic failure in narrow shear surfaces producing segmented chip [11]. Also, the high coefficient of thermal expansion of austenitic steels leads to serious difficulties in maintaining the machining tolerances. The high ductility favors development of built-up edge (BUE) in the tool, worsening the surface finish of the machined part [12].

The basic strategy to achieve an optimum machining is to select the adequate cutting speed and tool for each work material. In order to reach this objective, a good understanding of the effect that cutting speed has over mechanical and thermal properties of work material and cutting tool is necessary [13]. In this paper, the effect of cutting speed over tool wear, surface quality, cutting forces, and chip formation is analyzed when turning AISI 303 austenitic stainless steel. AISI 303 steel is one of the steels with enhanced machinability more frequently used for mass production in automatic lathes.

2 Experimental procedure

Machining tests were carried out using AISI 303 austenitic stainless steel. Table 1 shows the chemical composition for the tested steel. Machining operations were longitudinal turning, and part specimens were bars of 180-mm length and 60-mm diameter. Coolant was not employed in tests in order to analyze the behavior of stainless steels in dry machining. Dry machining satisfies the current trend of ecological machining [14] and at the same time it does not modify the results of the analysis of chemical composition in the tool surface.

2.1 Machining tests

Machining tests were performed modifying the cutting speed in a wide range: 37, 75, 150, 300, 450, 600 750,

Table 1 Chemical composition of AISI 303 work material

C	P	S	Si	Mn	Cr	Ni	Mo	Ti	N	Cu	Fe
0.050	0.033	0.273	0.365	1.776	17.773	8.783	0.271	0.003	0.041	0.273	70.392

845, and 870 m/min. That is, cutting speeds out of the range recommended by tool manufacturers (180–250 m/min) were tested. The objective was to analyze the effect of cutting speed over the work material–tool pair. Feed rate and depth of cut were kept constant at 0.2 mm/rev and 1 mm, respectively. These values are in recommended range as indicated by tool manufacturer. As formerly commented, these two parameters have not been modified due to the adverse effect over the surface finish and the cutting forces.

The tool was a multilayer-coated (TiCN, Al_2O_3, and TiN) cemented carbide cutting tool, submicrograin size with binder 8–10% of cobalt. It was a commercial grade insert with TNMG 160408 geometry.

The following variables were measured during the machining tests:

- The three components of cutting forces.
- Surface finish of machined surfaces.
- Superficial damage caused by the action of cutting.
- Tool wear.
- Geometrical features of chips.

The subsystem for measuring the cutting forces was composed of a triaxial Kistler 9121 piezoelectric dynamometer, a Kistler charge amplifier type 5070A, a DapBoard/2000 PCI data acquisition board and a computer data acquisition software (DasyLab). The forces registered were the feed force (F_f), the radial force (F_r), and the tangential cutting force (F_t). Measurements were recorded along the 125-mm length of machining on the 60-mm diameter pass.

Surface roughness (R_a) was measured over the machined surfaces using a Hommelwerke class 1 perfilometer, model Tester T4000. Cut-off was 0.8 mm and sampling length was 4.8 mm, according to ISO 13565-2:1997 standard.

A small portion of the machined surface was extracted to create samples for metallographic observation. These samples were mechanically polished and later on electrolytically polished with 10% oxalic acid solution at 6 VDC, 0.5 A, in order to reveal their microstructure. The microstructures were examined using an Olympus BX 80 metallographic microscope. Optical inspection of the machined surface was performed using a Jeol 6100 scanning electron microscope (SEM).

The worn cutting tools and the generated chips were also examined by SEM. Energy-dispersive spectrometry (EDX) techniques were used to measure the chemical compositions of the worn surfaces in the cutting tool.

3 Results and discussion

This section shows the results obtained from the analysis of measured values for cutting forces, condition of machined surface, tool wear, and chip morphology. The results are discussed to explain the effect of cutting speed in the turning of AISI 303 austenitic stainless steel.

3.1 Cutting forces

The evolution of the tangential force (F_t), feed force (F_f), and radial force (F_r) components is showed in Fig. 1 as a function of cutting speed. The tangential force component is approximately two times the two other force components. It should be noted that when cutting speed increases from 35 to 450 m/min, the three force components reduce and then they increase again with cutting speed. This behavior has also been observed in the machining of titanium alloys [15] and medium carbon steels [16].

The change in the evolution of cutting forces with cutting speed can be explained for the balance between the strain hardening rate and the thermal softening. These factors are already considered in the well-known law of Johnson–Cook (1) that explains the viscoplastic behavior of materials. This law expresses the flow stress (σ) as a function of the strain (ϵ), the strain rate ($\dot{\epsilon}$), and the temperature (T).

$$\sigma = \left(\sigma_0 + B\epsilon^n\right)\left(1 + C\ln\frac{\dot{\epsilon}}{\dot{\epsilon}_0}\right)\left(1 - T^{*m}\right) \tag{1}$$

In the first part of the curve in Fig. 1 (below 400–450 m/min), the cutting forces decrease with the increase of cutting speed. In this case, the thermal

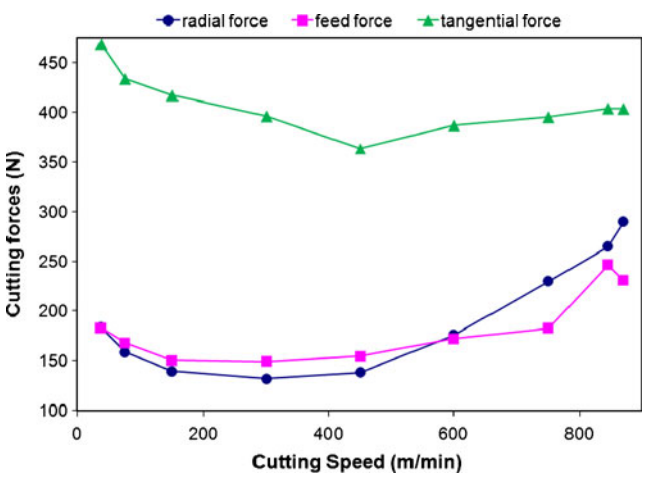

Fig. 1 Evolution of cutting forces with cutting speed

Table 2 Arithmetic average surface roughness (R_a) and maximum peak to valley height (R_t)

V (m/min)	37	75	150	300	450	600	750	845	870
R_a (μm)	*2.21*	1.84	2.00	2.14	2.12	**1.66**	*2.17*	1.84	1.90
$R_{a_{max}}-R_{a_{min}}$	1.50	0.58	1.11	0.74	0.26	0.16	0.11	0.15	1.05
R_t (μm)	*19.56*	9.50	10.77	10.47	10.91	**8.84**	*13.02*	10.45	12.61
$R_{t_{max}}-R_{t_{min}}$	10.20	3.28	8.36	5.96	5.62	1.49	8.26	2.93	6.27

In bold the minimum values achieved
In italics the maximum values achieved

softening factor ($1-T^{*m}$) predominates in the Johnson–Cook's equation. Due to the low thermal conductivity of the AISI 303 steel (15 W/mK), the heat generated in the machining cannot be dissipated quickly. This phenomenon causes an important increment in the temperature of the deformation areas and, consequently, the thermal softening of the work material; therefore the decrease of cutting force components takes place.

In the second part of the curve (Fig. 1) above 450 m/min, the cutting forces have a tendency to augment with the increase of the cutting speed. Now, the strain hardening rate factor $\left(\left(1+C\ln\frac{\dot{\epsilon}}{\dot{\epsilon}_0}\right)\right)$ predominates in the Johnson–Cook's equation. At these very high cutting speeds the strain rate is high, around 105 s^{-1}; the significant sensibility of stainless steels to the strain rate leads this factor to be predominant over the thermal softening and, in consequence, the cutting forces have a tendency to increase. This tendency agrees with the classic theory exposed by Oxley that considers the effect of strain hardening, strain rate and temperature on the properties of materials [17].

The behavior showed by the three cutting force components in the first part of the curve is similar. A reduction around 25% is observed for the three components. However, for cutting speeds above 450 m/min the slope of the curve is different in the three components. The tangential component experiences the smallest increment, around 10%. The feed component is the one which shows a quicker increment with a 52%, whereas the radial component is featured by a 40%. So, for cutting speeds above 600 m/min the value of the feed component overpass the value of the radial component. The effect of this behavior over tool wear and material side flow will be explained in Section 3.3.

3.2 Analysis of machined surface

3.2.1 Analysis of surface roughness

The effect of cutting speed on surface finish is analyzed in this section. Table 2 shows the values obtained for the average surface roughness (R_a) and the maximum peak to valley height (R_t) in the machined surface for different cutting speeds. These values are calculated as the average of six measurements.

Theoretical values of R_a and R_t can be estimated by means of Eqs. 2 and 3, respectively. According to them, the roughness values for the cutting conditions used in the machining tests are 1.5 and 6.25 μm, respectively. These ideal values for R_a and R_t are lower than the real ones as measured by the perthometer. The reason is that surface finish is affected by additional factors related to machining stability, work material, tool wear or machining conditions [25].

$$R_a = 0.0321\frac{f^2}{r_\epsilon} \tag{2}$$

$$R_t = \frac{1}{8}\frac{f^2}{r_\epsilon} \tag{3}$$

It can be observed that the surface machined at 600 m/min shows the lowest R_a (1,66 μm) and R_t (8,84 μm) values. The surfaces machined at 37 and 750 m/min are featured by higher R_a and R_t values. These high values are due to vibrations (unstable machining) during the operation. When analyzing the values of the cutting force components, it was observed that variation of signal amplitude ($F_{max}-F_{min}$) is max-

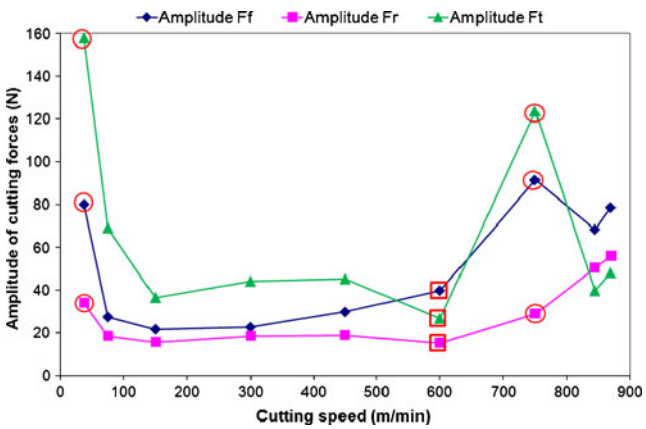

Fig. 2 Evolution of the amplitude of cutting forces with cutting speed

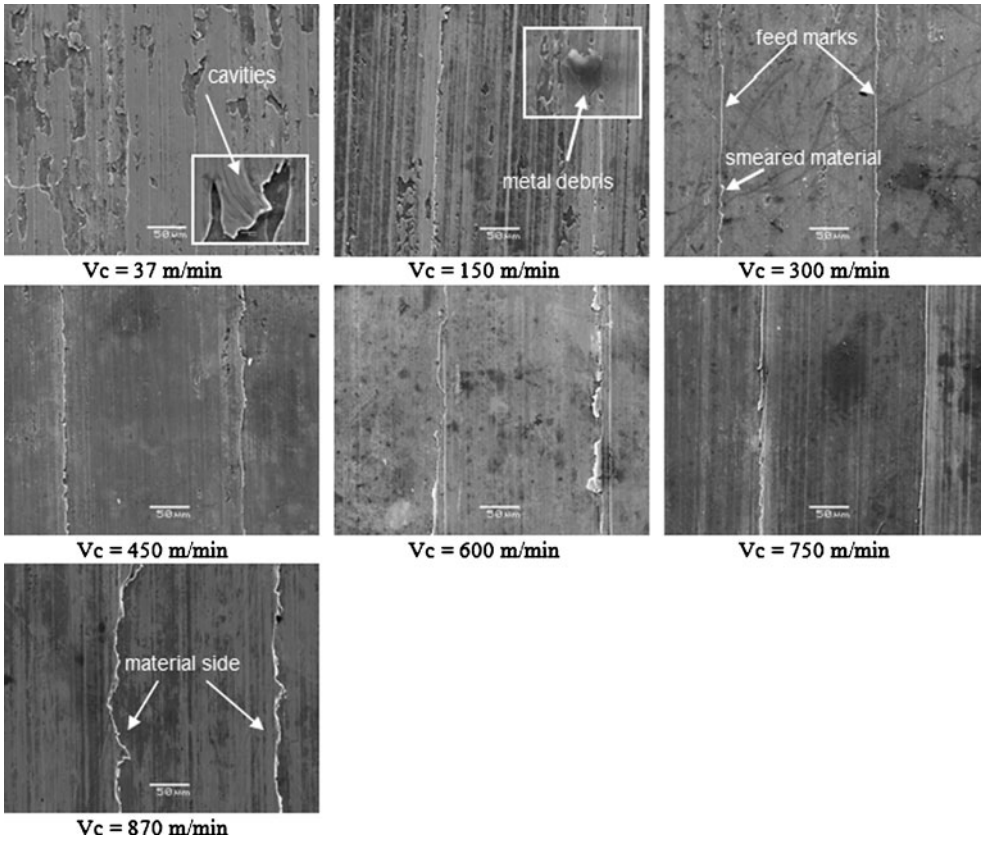

Fig. 3 SEM micrographs of machined surfaces at different cutting speed

imum for the three components at 37 and 750 m/min; this fact gives an idea of the instability of the cutting operation at these cutting speeds. Meanwhile, the minimal amplitude is reached at 600 m/min (Fig. 2), which means stable machining and also minimal roughness, as indicated before. This fact corroborates the idea that roughness depends on cutting parameters and tool vibrations [18, 19].

3.2.2 Analysis of surface damage

SEM micrographs of machined surfaces at different cutting speeds are shown in Fig. 3. The influence of cutting speed in surface finish is confirmed with these images. Surfaces machined at low cutting speeds (37 to 300 m/min) show cavities, metal debris and feed marks with smeared material particles. Surfaces machined at high cutting speeds (450 to 870 m/min) do not contain cavities nor metal debris, but they show evidence of material side flow. Similar effects were reported by other authors during machining of modified AISI 420 stainless steel [20]. The material side flow takes place when the chip material in the cutting tool edge is exposed to high pressure and temperature. This state produces a complete plastification of the material, that flows through the main cutting edge toward the secondary cutting edge and it adheres to the new machined surface.

Kishawy and Elbestawi [21] researched two mechanisms for material side flow. In the first mechanism, the material is squeezed between the tool flank face and the machined surface when chip thickness is below a minimum value. In our research, when considering the evolution of chip thickness with cutting speed (Fig. 4), it can be observed that above 450 m/min the material side flow becomes more evident and the chip thickness suffers a significant reduction.

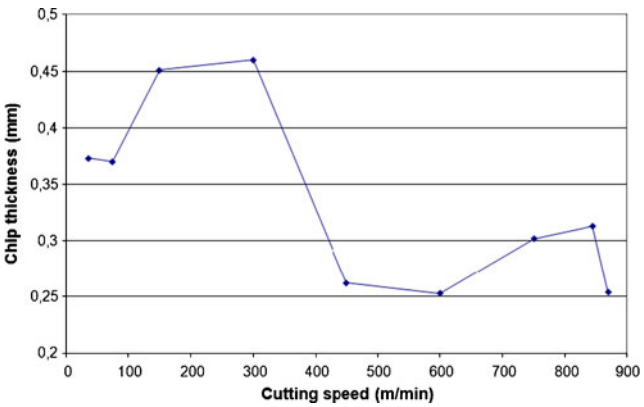

Fig. 4 Evolution of chip thickness with cutting speed

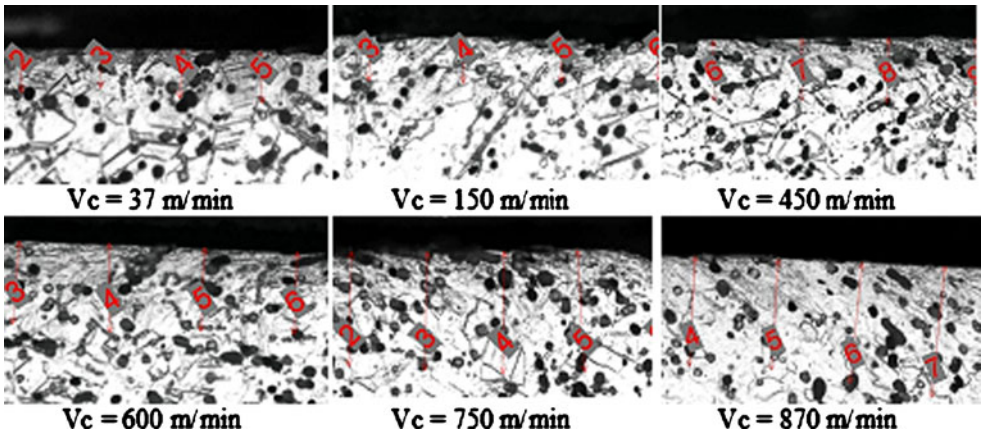

Fig. 5 Depth of deformed microstructure of machined specimens at different cutting speeds

In the second mechanism, the plastified material in the cutting zone flows through the worn trailing edge to the side of the tool. In Section 3.3, where tool wear is analyzed, severe wear is observed on the trailing edge at cutting speeds above 450 m/min and material side flow is evident.

In addition, some authors [22, 23] have demonstrated that cutting speed has a significant influence on material side flow. The high temperature generated during high-speed machining helps to the material plastification and, hence, a tendency for material side flow.

The effect of cutting speed on the structural change in the work material was analyzed. A transversal cutting was done to the machined specimen and the disk surfaces were electrolytically polished and prepared for analysis in metallographic microscopy. The images in Fig. 5 show the deformation of the grains in the machined surface. Depth of the deformed area was estimated using ten measurements along the transversal section. This analysis was carried out for different cutting speeds; Table 3 contains the mean values. The results show an increase in the depth of the deformed area with the increase of cutting speed, due to the strain hardening which features the austenitic stainless steels.

3.3 Analysis of tool wear

The surface of the cutting tools used for the machining tests was analyzed using the SEM and EDX techniques to determine the nature of wear. Cutting tools were multilayer coated cemented carbide inserts (TiCN–Al_2O_3–TiN). Many authors have been carried out different studies to evaluate the effect of tool coatings on the cutting process, such as Ucun and Aslantas [24] summarize in recent times. The aluminum oxide (Al_2O_3) coating provides chemical stability minimizing the wear by diffusion and, at the same time, it improves the strength to abrasive wear. The titanium nitride (TiN) coating reduces the coefficient of friction on the tool rake face [25]. The TiCN coating improves the adherence of the coatings to the substrate of the insert.

The EDX analysis of components in a new insert shows high levels of the original coating elements (TiCN–Al_2O_3–TiN). On the contrary, the analysis of worn inserts shows higher levels of iron (Fe), chromium (Cr), silicon (Si), nickel (Ni), sulfur (S) and manganese (Mn) (Fig. 6). As mentioned before in Table 1,

Table 3 Work-hardening measures carried out in the transversal section of the machined specimens at different cutting speeds

V (m/min)	37	150	450	600	750	870
Distance from surface(μm)	2.18	1.84	3.16	3.57	5.11	6.05

	New tool		Worn tool	
Element	Weight%	Atomic%	Weight%	Atomic%
C K	7.50	12.37	5.51	11.00
N K	31.82	44.97	10.82	18.53
O K	18.19	22.51	24.21	36.31
Al K	8.15	5.98	14.70	13.07
S K	-	-	0.21	0.16
Ti K	34.25	14.15	23.83	11.94
Cr K	-	-	4.15	1.91
W	0.09	0.01	-	-
Mn K			0.56	0.24
Fe K			14.39	6.18
Ni K			1.64	0.67
Totals	100.00		100.00	

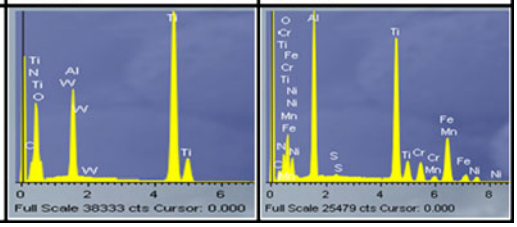

Fig. 6 EDX chemical composition analysis at flank face for new and worn cutting tools

these elements are alloying elements for the AISI 303 austenitic stainless steel. As it is known, these work material components are located in the flank and rake faces of the cutting tool and they are called BUE and built-up layer, respectively [26].

On the other hand, Fig. 7 shows layers of material adhered to the tool flank face. A quantitative element mapping was carried out using EDX analysis to characterize the components attached to the flank surface. The mapping results indicated that these layers were composed by iron (Fe), chromium (Cr), nickel (Ni), and manganese (Mn) which come from the workpiece material. When machining in the range of low cutting speeds (37–300 m/min) these layers are located close to the main cutting edge and they spreads over the flank face. When machining at high speeds (above 300 m/min), a tendency to form lumps of FeCr welded to the main edge can be observed. With the increment of cutting speed the lumps tend to displace toward the secondary edge, as it can be appreciated in Fig. 8 for a cutting speed of 870 m/min.

As supposed, increase of cutting speed implies a more severe tool wear rate. Besides, the wear band in the tool displaces from the main edge toward the secondary edge. In Fig. 8, it is observed how wear is more accused in the region near to the tool nose radius for a cutting speed of 300 m/min, whereas for cutting speeds of 845 and 870 m/min the most worn region is observed at the secondary edge. This wear in the secondary edge favors material side flow at the highest cutting speeds, as it was indicated previously in Section 3.2.2.

Micrographs of tool rake face for worn tools (zone A in Fig. 9c) and spectral information obtained with EDX analysis (zone A in Fig. 10) show higher levels of sulfur

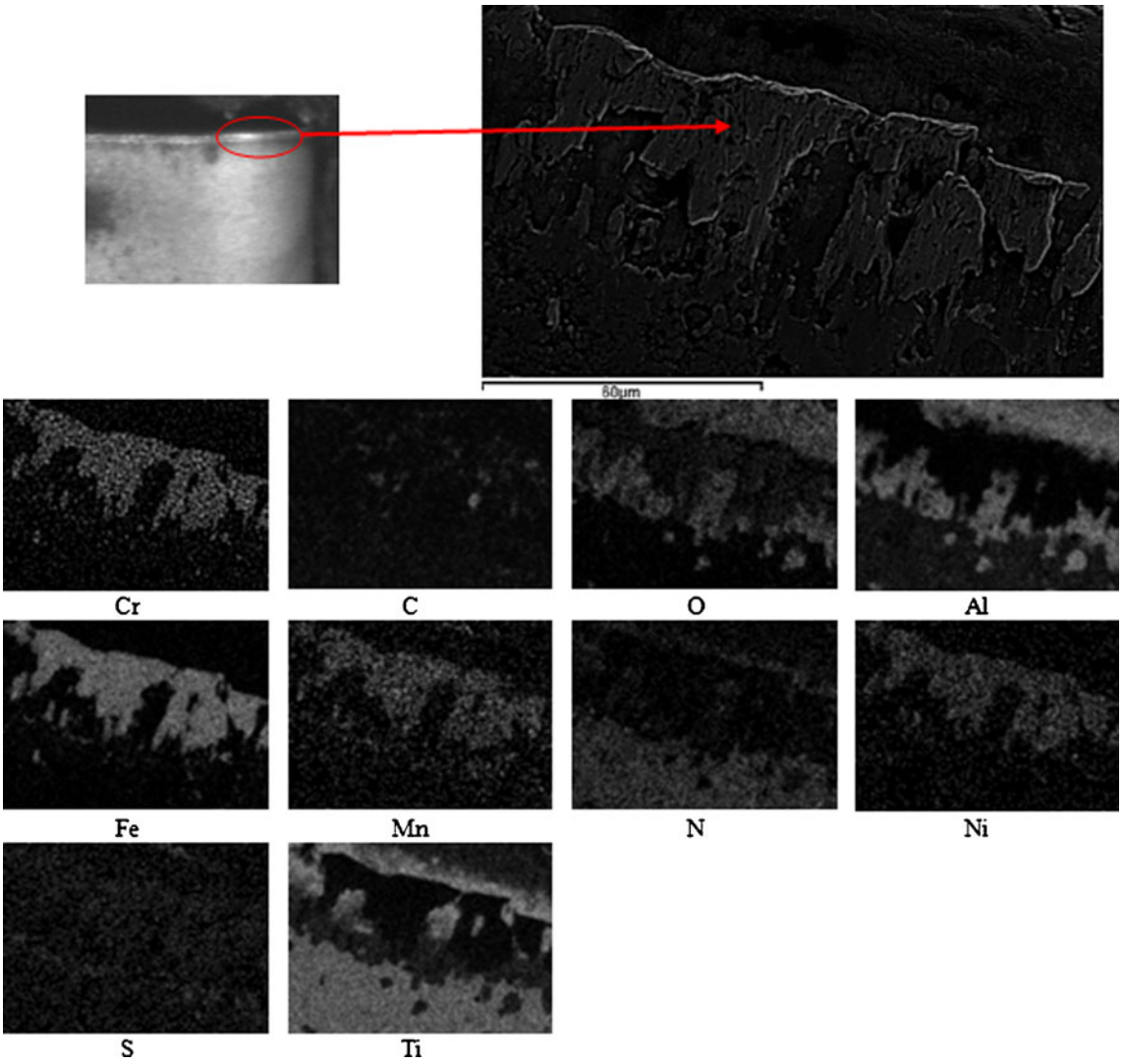

Fig. 7 SEM mapping image for adhered material in the tool flank face

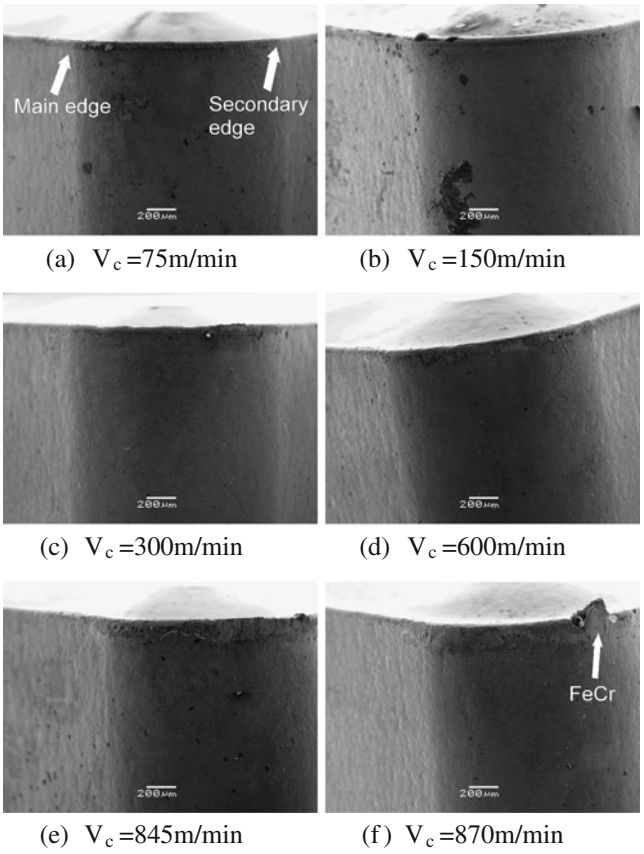

(a) V_c =75m/min (b) V_c =150m/min

(c) V_c =300m/min (d) V_c =600m/min

(e) V_c =845m/min (f) V_c =870m/min

Fig. 8 SEM images for tool flank wear at several cutting speeds

(S) and manganese (Mn), which indicates the presence of MnS layers.

This MnS layer is uniform through the tool rake face at low or medium cutting speeds. This layer acts like a barrier for adhesive wearing and it prevents from welding or stiffening of work material in the tool surface. At high cutting speeds the MnS layer in the tool rake face is more irregular, since higher temperatures caused by higher cutting speeds makes this layer viscous and unstable. This layer spreads also toward the inner of the tool moving away from the edge border without reaching the secondary edge. This effect leaves the cutting edge unprotected and, consequently, welding of work material on the tool edge border takes place.

In the areas of tool rake face not protected by the MnS layer (zone B in Fig. 9c) high content of tungsten (W) and cobalt (Co) (from substrate) and low percentages of aluminum (Al), titanium (Ti), and nitrogen (N) (from coating) are observed (zone B in Fig. 10). This analysis indicates that tool coating has disintegrated by diffusion wearing which occurs at high cutting temperatures.

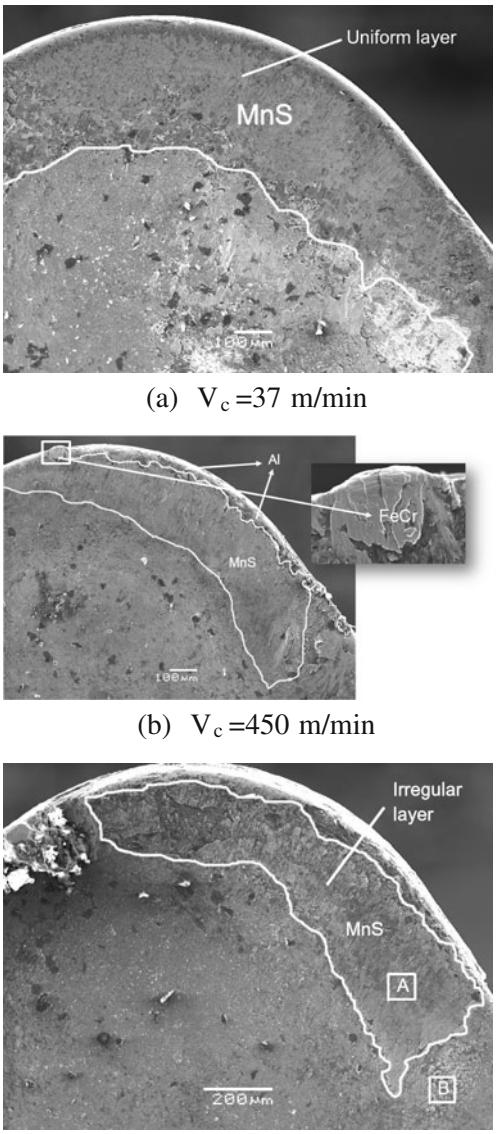

(a) V_c =37 m/min

(b) V_c =450 m/min

(c) V_c =870 m/min

Fig. 9 SEM images in the crater region at several cutting speeds

3.4 Analysis of chip formation

A morphological analysis of chips was carried out at different cutting speeds with the purpose of studying the influence of cutting speed in the formation mechanism of the chip. Chips were analyzed by means of optic and scanning electron microscopy. In all the cases chips were segmented type, but geometrical differences were observed as consequence of cutting speed variation. Segmented chip is formed due to some features of austenitic stainless steels, as high work-hardening rate and low thermal conductivity which prevents heat

	Zone A		Zone B	
Element	Weight%	Atomic%	Weight%	Atomic%
C K	13.85	26.20	12.74	30.93
O K	32.01	45.44	18.25	33.28
Al K	8.98	7.56	5.57	6.02
Si K	0.29	0.24	-	-
S K	1.20	0.85	1.26	1.15
Ca K	0.19	0.11	0.18	0.13
Ti K	26.36	12.50	21.78	13.26
Cr K	4.24	1.85	4.64	2.60
Mn K	4.94	2.04	2.27	1.20
Fe K	7.12	2.90	14.00	7.31
Co K	-	-	1.51	0.74
Ni K	0.81	0.32	1.58	0.79
W M	-	-	16.21	2.57
Totals	100.00		100.00	

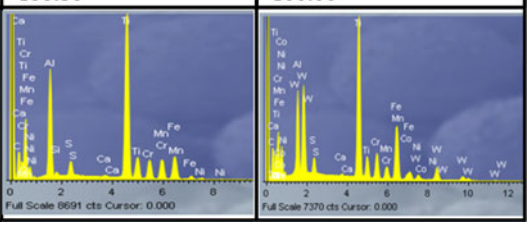

Fig. 10 EDX chemical composition analysis at the crater area of Fig. 9c

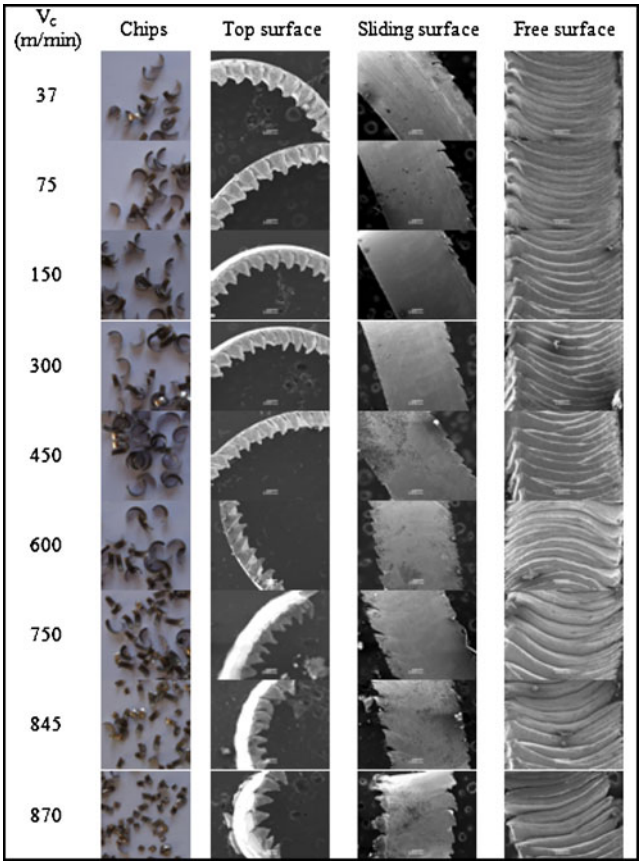

Fig. 11 SEM images of chips at several cutting speeds

evacuation. The heat concentrates around the shear zone and it produces thermal softening and flow stress reduction in work material. This effect produces adiabatic bands of deformation that leads to local deformation in a nearly plane area.

Ten samples of chip were considered at each cutting speed so that the results of geometrical analysis were representative. Moreover, for each chip sample three images were acquired using SEM to measure its thickness and width and to analyze the morphology of the free surface and the slipping surface (the one in contact with the tool rake face). Figure 11 shows an example of chip images at different cutting speeds. The first column indicates that as higher the cutting speed smaller the chip length, which is more significant above 600 m/min. This is due to severe segmentation that occurs at high cutting speeds which produces the breaking of chip in lamellas.

Free surface of chip is featured by a rough aspect. For all cutting speeds, a lamellas pattern is observed as result of slipping mechanism. Lamellas are smaller and more uniform for low cutting speeds, as it can be observed in the last column in Fig. 11. With the increase of cutting speed the lamella pattern is deeper, which indicates higher chip segmentation.

As it is well-known in literature [27], chip surface that slips on the tool rake face during cutting process is subjected to high pressure and friction force, which leads to very high cutting temperatures (around 1.200°C). Combination of these effects produces in this chip sliding surface a flat and bright aspect. Chip width measurements were carried out using the chip sliding surface images. Chip width varies from 1.174 (at 37 m/min) to 1.701 mm (at 870 m/min) with the increase of cutting speed. It can be concluded from these measures that lateral chip material flow takes place, which is higher with the increase of cutting speed due to the higher pressures and temperatures in the chip.

It is also observed that chips produced at low cutting speeds (under 300 m/min) are featured by discontinuities in one of the lateral borders. However, at cutting speeds above 300 m/min cracks and discontinuities appear in both lateral borders (Fig. 12) due to severe deformation that occurs at these very high cutting speeds.

EDX analysis was carried out on the chip sliding surface. Results show that they are not elements of tool coating or its substrate. This lets us conclude that there was no transference of material from the tool toward the chip, that is, there was no diffusion wearing.

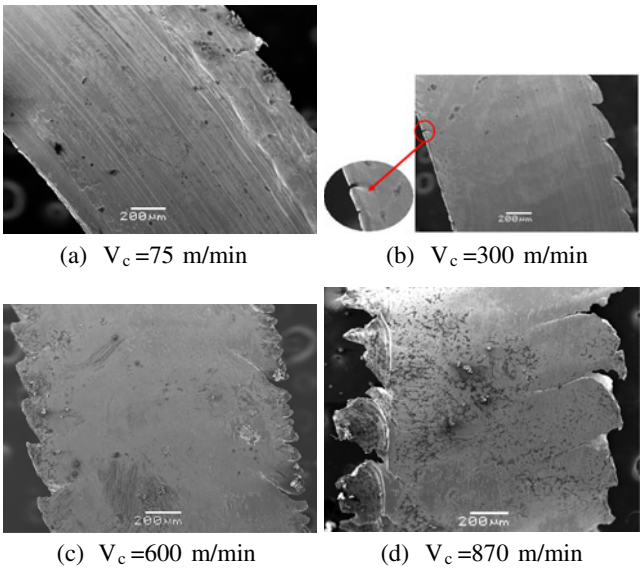

(a) V_c =75 m/min (b) V_c =300 m/min

(c) V_c =600 m/min (d) V_c =870 m/min

Fig. 12 Chip sliding surface at several cutting speeds

Chip thickness was measured as the average of ten chip images acquired at each cutting speed. Figure 4 shows the relation between chip thickness (h_c) and cutting speed. It is observed that above 450 m/min chip thickness decreases significantly. In the research carried out by Kishawy and Elbestawi [21], the authors concluded that when chip thickness reaches a minimum value the material is squeezed between the tool flank face and the machined surface and material side flow is observed. In our study, this phenomenon takes place when chip thickness in inferior to 0.35 mm at cutting speeds above 450 m/min, as it is indicated in Fig. 3.

Chip thickness is related to the shear angle by means of the following expressions stated in the classic Merchant's theory (4):

$$r_c = \frac{h}{h_c} \qquad \phi = \tan^{-1}\left(\frac{r_c \cos\alpha}{1 - r_c \sin\alpha}\right)\frac{f^2}{r} \tag{4}$$

where r_c is the chip compression ratio, h is the uncut chip thickness, ϕ is the shear angle, and α is the tool rake angle. When cut chip thickness (h_c) is smaller, the chip compression ratio and the shear angle become higher. High values of ϕ and r_c correspond to small chip deformation and less consumed energy, therefore favoring the cutting process.

Table 4 shows the values for r_c and ϕ calculated using the Merchant's theory. For cutting speeds under 450 m/min, the chip compression ratio is below 0.5 and it approximates to 0.7–0.8 for higher cutting speeds. The shear angle presents a similar behavior, that is, it stays always close to 30° at cutting speeds under 450 m/min and takes values near to 40° when cutting speed is higher than 450 m/min. This behavior has already been observed in other materials, such as Inconel 718. Thakur et al. [28] observed that a higher cutting speed increases the shear angle, which results in a shorter shear plane for a fixed shear strength. The authors concluded that when the shear angle increases, thin chips are generated, speed of chips is higher, and the result is a reduction of cutting force and friction.

Table 4 Values for chip thickness, chip compression ratio, and shear angle at different cutting speeds

V_c(m/min)	h(mm)	h_c(mm)	r_c	ϕ(degrees)
37	0.199	0.373	0.536	29.56
75	0.199	0.370	0.540	29.77
150	0.199	0.451	0.443	24.88
300	0.199	0.460	0.435	24.43
450	0.199	0.262	0.763	39.70
600	0.199	0.253	0.790	40.79
750	0.199	0.302	0.662	35.43
845	0.199	0.313	0.639	34.39
870	0.199	0.254	0.787	40.67

4 Conclusions

Behavior of austenitic stainless steels has been researched when machining at very high cutting speeds in dry turning. In this paper, the behavior of workpiece material and cutting tool is analyzed at cutting speeds much higher than the speeds used by other researchers. Usual cutting speeds are in the range of 200 to 300 m/min and use of coolant is extensive for these materials. In this research, very high cutting speeds of up to 870 m/min were tested. These machining conditions were considered for economical and ecological reasons, in accordance to actual state of technology. The effect of very high cutting speeds was analyzed over cutting forces, quality surface, tool wear and chip geometry.

From the results obtained, a critical cutting speed of 450 m/min is identified. Above this critical cutting speed, the behavior of machined material changes with regard to lower cutting speeds. Traditionally, stainless steels are machined at cutting speeds between 150–300 m/min. However, this research concludes that these materials have a good behavior at higher speeds. For example, the main component of cutting forces (F_t) reduces above 450 m/min, which implies less power consumption and less stress and deformation in cutting tool. Besides, with regard to the surface of the machined workpiece, the roughness achieved at these very

high cutting speeds is similar to the one at lower cutting speeds, reaching the R_a minimum value at 600 m/min. No cavities were found nor any metal debris; however, material side flow is observed above the critical cutting speed. Depth of the zone affected by microstructural change increases with cutting speed; however, the values obtained are acceptable for all the tested cutting speeds. The analysis of chip also shows that a significant change in chip geometry is obtained above the critical cutting speed of 450 m/min; chip thickness is significantly less, which implies lower chip compression ratio and higher shear angles. These parameters are indicative of the good behavior of austenitic stainless steels to dry machining at very high cutting speeds.

The study concludes that there is an unexplored range of cutting speeds very interesting for high-performance machining, where the behavior of workpiece material is very favorable although tool wear is high. Nevertheless, nowadays cost of tool inserts can be considered secondary when compared with other operation costs, for instance the machine hourly cost for high-end multitasking machines.

Acknowledgements We gratefully acknowledge the financial support provided by the Spanish R2-TAF initiative through a researcher mobility grant.

References

1. Schulz H (1996) Hochgeschwindigkeitsbearbeitung—high speed machining. Hanser Fachbuchverlag. ISBN 978-3446187962.
2. Puertas I, Luis, CJ (2003) Surface roughness prediction by factorial design of experiments in turning processes. J Mater Process Technol 143-144:390–396
3. Pawade RS, Joshi SS, Brahmankar PK, Rahman M (2007) An investigation of cutting forces and surface damage in high-speed turning of Inconel 718. J Mater Process Technol 192–193:139–146
4. Cakir MC, Ensarioglu C, Demirayak I (2009) Mathematical modeling of surface roughness for evaluating the effects of cutting parameters and coating material. J Mater Process Technol 2009–1:102–109
5. Chen L, Du Y, Yin F, Li J (2007) Mechanical properties of (Ti,Al)N monolayer and TiN/(Ti,Al)N multilayer coatings. Int J Refract Met Hard Mater 25–1:72–76
6. Platit (2002). http://www.platit.com/open-source
7. Schulz H, Abele E, Sahm A (2001) Materials aspects of chip formation in HSC machining. Annals of the CIRP 50/1:45–48
8. Nalbant M, Altm A, Gokkaya H (2007) The effect of previous term cutting speed and cutting next term tool geometry on machinability properties of nickel-base Inconel 718 super alloys. Mater Des 28:1334–1338
9. Paro J, Hänninen H, Kauppinen V (2001) Tool wear and machinability of HIPed P/M and conventional cast duplex stainless steels. Wear 249:279–284
10. Maranhao C, Davim JP (2010) Finite element modelling of machining of AISI 316 steel: numerical simulation and experimental validation. Simulation Modelling Practice and Theory 18:139–156
11. Dolinsek S (2003) Work-hardening in the drilling of austenitic stainless steels. J Mater Process Technol 133: 63–70
12. Korkut I, Kasap M, Ciftci I, Seker U (2004) Determination of optimum cutting parameters during machining of AISI 304 austenitic stainless steel. Mater Des 25:303–305
13. Dagiloke IF, Kaldos A, Douglas S, Mills B (1995) High-speed machining: an approach to process analysis. J Mater Process Technol 54:82–87
14. Leppert T (2011) Effect of cooling and lubrication conditions on surface topography and turning process of C45 steel. Int J Mach Tools Manuf 51:120–126.
15. Sun S, Brandt M, Dargusch MS (2009) Characteristics of cutting forces and chip formation in machining of titanium alloys. Int J Mach Tools Manuf 49:561–568
16. Sutter G, Molinari A (2005) Analysis of the cutting force components and friction in high speed machining. J Manuf Sci Eng 127:245–250
17. Oxley PLB (1989) The Mechanics of Machining: An Analytical Approach to Assessing Machinability. Ellis Horwood Ltd., England
18. Lu C, Ma N, Chen Z, Costes J-P (2010) Pre-evaluation on surface profile in turning process based on cutting parameters. Int J Adv Manuf Technol 49:447–458
19. Abouelatta O B, Mádl J (2001) Surface roughness prediction based on cutting parameters and tool vibrations in turning operations. J Mater Process Technol 118:269–277
20. Liew WYH, Ngoi BKA, Lu YG (2003) Wear characteristics of PCBN tools in the ultra-precision machining of stainless steel at low speeds. Wear 254:265–277
21. Kishawy HA, Elbestawi MA (1999) Effects of process parameters on material side flow during hard turning. Int J Mach Tools Manuf 39:1017–1030
22. Warnecke G, Bach P (1988) Mechanical and material influences on machined surface in precision turning of steel with ceramics. In: Proceedings 16th North American Research Conference. pp 209–216
23. El-Wardany TI, Mohamed E, Elbestawi MA (1993) Material side flow in finish turning of hardened steel with ceramic tools. ASME. pp 159–170
24. Ucun I, Aslantas K (2010) Numerical simulation of orthogonal machining process using multilayer and single-layer coated tools. Int J Adv Manuf Technol (accesible online) doi:10.1007/s00170-010-3012-9
25. Ciftci I (2006) Machining of austenitic stainless steels using CVD multi-layer coated cemented carbide tools. Tribology 39:565–569
26. Hamann JC, Le Maitre F, Guillot D (1994) Selective transfer Built-up Layer displacement in high-speed machining—consequences on tool wear and cutting forces. Annals of the CIRP 43/1:69–72
27. Zhang S, Guo YB (2009) An experimental and analytical analysis on chip morphology, phase transformation, oxidation, and their relationships in finish hard milling. Int J Mach Tools Manuf 49:805–813
28. Thakur DG, Ramamoorthy B, Vijayaraghavan L (2009) Machinability investigation of Inconel 718 in high-speed turning. Int J Adv Manuf Technol 45:421–429